Dose distributions of high-precision radiotherapy treatment: A comparison between the CyberKnife and TrueBeam systems

M. Ito[1*], T. Kawamura[1], Y. Mori[1], T. Mori[1], A. Takeuchi[1], Y. Oshima[1], K. Nakamura[1], T. Aoyama[1], N. Kaneda[1], T. Ishiguchi[1], S. Mizumatsu[2]

[1]*Department of Radiology, Aichi Medical University, Yazako-Karimata, Nagakute, Aichi, Japan*
[2]*CyberKnife Center, Aoyama General Hospital, Aichi, Japan*

ABSTRACT

► *Original article*

Corresponding authors:
Makoto Ito, M.D.
Fax: +81 561 63 3268
E-mail:
itou.makoto.292@mail.aichi-med-u.ac.jp

Background: Several high-precision stereotactic radiation therapy modalities are currently used in clinical settings. We aimed to evaluate whether the CyberKnife (CK) or TrueBeam (TB) radiation treatment systems were more appropriate for treating targets of various morphologies according to the physical properties of each device. **Materials and Methods**: Spheres (diameter = 5–50 mm), as well as triangular prisms and cubes (length of a side = 10–50 mm), were used as virtual targets for each treatment delivery system. A phantom with dosimetry film was irradiated to evaluate the flatness and gradient of the radiation treatment from each modality. **Results:** The homogeneity index (HI) for the spherical targets was significantly higher (dose distribution was more homogeneous) using the TB than when using the CK (1.9 vs. 1.4; p = 0.002). There were no significant differences between treatment modalities in the HI for more complex shapes. The HI increased monotonically as the virtual target diameter increased for the CK (p = 0.048). The flatness parameter was lower for the TB than for the CK (1.4 vs. 1.1; p < 0.001). **Conclusion:** The CK is particularly robust for delivering therapeutic radiation to small targets, while the TB is more suitable for targets with a simple shape or when the HI is a critical treatment factor.

Keywords: *Cyberknife; TrueBeam; homogeneity index; conformity index.*

INTRODUCTION

Stereotactic radiation therapy (SRT) has been widely used to treat various types of tumours in Western countries and Japan [1]. Several SRT modalities are currently available in clinical practice, including individual institutions and group affiliation facilities [2]. For optimal therapy, the treatment device should be selected according to the histological type, size, and shape of the target lesion(s). In this study, we conducted a dosimetric comparison between the CyberKnife II (CK; Accuray, Sunnyvale, CA, USA) and the TrueBeam STx (TB; Varian Medical Systems, Tokyo, Japan). These 2 modalities use different radiation delivery methods: the CK has a robot-controlled 6-MV linear accelerator

(LINAC) for non-isocentric, cone-collimated beams [3], and the TB delivers radiation to the isocentre using dynamic conformal arcs (DCAs). The effectiveness and safety of TB with a flattening filter-free (FFF) beam has been previously demonstrated [4]. Although multiple studies have compared the clinical characteristics of these treatment devices [5-10], none have evaluated and compared their physical properties in detail using simulated targets. The objective of this study was to investigate the physical properties of the CK and TB systems and compare them with respect to various target morphologies to obtain basic information about the appropriate clinical indications of each device.

MATERIALS AND METHODS

This study consisted of 2 parts. First, the dose distributions of the CK and TB were compared in simulation planning for virtual objects of various shapes and sizes in a cubic phantom. Second, the dose profiles from phantom irradiations were verified using film dosimetry for quality assurance.

Planning systems

Radiotherapy treatment was planned with MultiPlan® version 5.2.1 (Accuray, Sunnyvale, CA, USA) for the CK and iPlan RT (iPlan RT Image and iPlan RT Dose) version 4.5.3 (BrainLAB, Munich, Germany) for the TB. For the CK, the non-isocentric, non-coplanar, conformal, and inverse-planning technique was used. In addition, 6–45 nodes (17–83 beams) were employed for the CK. Since the CK does not have a multi-leaf collimator, the diameter of the collimator (5–40 mm) was selected based on target size and shape. The ray-tracing method was used for the dose calculation algorithm. Optimization calculations were repeated until a favourable dose distribution was obtained. For the TB, the DCA technique with 4 arcs and a 6-MV, FFF beam and a 2.5-mm micro-multileaf collimator system were used. This setting provides irradiation at a rate of 1400 MU/min. The calculation grid was 2 mm, and the pencil-beam dose calculation algorithm was used. Moreover, the angle spread and range of gantry rotation for the TB were manually adjusted to obtain the optimal plan. In most cases, the spread angle and arc range were 135° and 120°, respectively.

Target objects

Simple round objects (spheres) and angled objects (cubes and triangle prisms) were used as virtual targets for simulation planning. The cube was a regular hexahedron and the triangle prism was shaped similar to an isosceles right triangle. Six spheres (diameter = 5, 10, 20, 30, 40, and 50 mm), as well as 5 cubes and 5 triangular prisms (length of a side = 10, 20, 30, 40, and 50 mm), were prepared as simulation targets for

each planning system.

For each target, optimal plans were prepared using a multifocal beam entry system for the CK and a 4-arc DCA for the TB. The leaf margin was set at 0 mm for the TB. The prescription dose of 600 cGy (100% dose) was set to cover 95% of the target volume. Thirty-two simulation plans were prepared: 16 for the CK and 16 for the TB.

Comparison of dose distributions

The maximum, minimum, and mean target doses; conformity index (CI); and homogeneity index (HI) for the 2 methods were compared. The indices were defined by the equations 1 and 2:

$$CI = Paddick\ CI = (TV_{PIV})^2/(TV \times PIV), \tag{1}$$

Where; TV_{PIV} is the target volume covered by the prescription isodose volume, TV is the target volume, and PIV is the prescription isodose volume [11].

$$HI = D_{max}/D_{min}, \tag{2}$$

Where; D_{min} is the minimum dose and D_{max} is the maximum dose, for both doses within the target volume [12].

The beam-on-time was calculated for a radiation delivery rate of 600 mU/min in the CK and 1400 mU/min in the TB.

Verification and comparison of dose profiles

A cubic, stereotactic, dose-verification phantom (I'mRT phantom; IBA Dosimetry, Schwarzenbruck, Germany), inserted with Gafchromic film EBT3 (Ashland, Covington, KY, USA), was irradiated based on the treatment plans from each planning system. The irradiated films were analysed using the SNC Patient™ film dosimetry system (Sun Nuclear Corporation, Melbourne, FL, USA). The standard for γ analysis was set at 3%/3 mm for a threshold of 30%. The clinically applicable pass rate was ≥90%. Sixty-four dose profiles along both the *x*- and *y*-axes at the centre of the irradiated area and 128 gradients on both the *x* and *y* sides of the film were analysed. Flatness and gradient were defined by equations 3 and 4:

$$Flatness = D_{max}/D_{95\%}, \tag{3}$$

Int. J. Radiat. Res., Vol. 16 No. 4, October 2018

396

where D_{max} is the maximum dose within the absorption curve and $D_{95\%}$ is 95% of the maximum dose ($D_{95\%}$ = 570 cGy).

$$\text{Gradient} = \Delta y/\Delta x. \qquad (4)$$

Gradient is the increase in the lower edge of a radiation field at 50% dose (300 cGy) to $D_{95\%}$ (570 cGy).

Statistical analysis

For dosimetric parameters, the Mann–Whitney *U*-test was used for categorical variables and both the *t*-test and Welch's test were used for continuous variables. One-way analysis of variance was used for multiple comparisons, and trends were analysed using the Jonckheere–Terpstra test. For dosimetric parameters, multivariate analysis was performed for both the HI and CI. If a stratified analysis was included, the data tended to show a difference in the univariate analysis. Therefore, all target characteristics were included as candidate variables. EZR (the R Foundation for Statistical Computing, Vienna, Austria, version 2.17.0) was used for all statistical analyses [13]. Statistical significance was set at $p < 0.05$.

RESULTS

Comparison of treatment plans

Table 1 shows the stratified dosimetric parameters for the CK and TB groups. The median dose coverage was 95.0% (range, 94.7–95.5%) for the CK and 94.2% (range, 90.5–100.0%) for the TB; there was no significant difference in these values ($p > 4.^{3\,3}4$). The minimum, mean, and maximum doses were higher for the CK than for the TB. The HI was better (i.e., the dose distribution was more homogeneous) for the TB than for the CK (2.1 ± 0.3 vs. 1.8 ± 0.4; $p = 0.043$). The HI for a simple shape (sphere) differed significantly between the TB and the CK (1.9 ± 0.3 vs. 1.4 ± 0.1; $p = 0.002$). However, when stratified analysis of the HI was performed for each shape, this difference became insignificant as the shape became more complex (cube: 2.1 ± 0.5 vs. 1.8 ± 0.1; $p = 0.259$; triangular prism: 2.2 ± 0.2 vs. 2.2 ± 0.1; $p = 0.970$) (table 2). Conversely, there was no difference in the CI between the TB and CK (0.8 ± 0.1 vs. 0.8 ± 0.1; $p = 0.194$), with similar results when a stratified analysis of the HI for each shape was performed. Irradiation time (in min) was significantly shorter for the TB than for the CK (1.0 ± 0.2 vs. 21.7 ± 4.7; $p < 0.001$).

Figure 1 shows comparisons of the HI and CI for different combinations of 2 shapes for both modalities. As the shapes became more complicated, the HI significantly decreased for the TB ($p < 0.001$), but no such significant difference was observed for the CK ($p = 0.542$).

For both treatment systems, the CI was more favourable for spheres than for triangular prisms ($p < 0.001$ and $p = 0.006$ for the CK and the TB, respectively), with the effect of target shapes on the CI being similar for both devices.

Table 1. Dosimetric parameters for the CK and the TB.

	CK	TB	
	(*n* = 16)	(*n* = 16)	*p*-value
Coverage median (25–75%)	95.0 (94.7–95.5)	94.2 (90.5–100.0)	0.99
Minimum dose (cGy)	486.2 ± 64.2	406.4 ± 84.3	0.005
Mean dose (cGy)	737.7 ± 35.6	636.7 ± 12.7	<0.001
Maximum dose (cGy)	973.6 ± 100.9	690.3 ± 16.8	<0.001
HI	2.1 ± 0.3	1.8 ± 0.4	0.043
CI	0.8 ± 0.1	0.8 ± 0.1	0.194
Beam-on-time (min)	21.7 ± 4.7	1.0 ± 0.2	<0.001

Values are presented as mean ± SD, unless otherwise specified.

CK, CyberKnife; TB, TrueBeam; SD, standard deviation; HI, homogeneity index; CI, conformity index.

397

Int. J. Radiat. Res., Vol. 16 No. 4, October 2018

Table 2. Results of stratified analysis of the HI and CI for each target shape.

		CK	TB	
		(mean ± SD)	(mean ± SD)	*p*-value
HI	All cases (*n* = 32)	2.1 ± 0.3	1.8 ± 0.4	0.043
	Sphere (*n* = 12)	1.9 ± 0.3	1.4 ± 0.1	0.002
	Cube (*n* = 10)	2.1 ± 0.5	1.8 ± 0.1	0.259
	Triangular prism (*n* = 10)	2.2 ± 0.2	2.2 ± 0.1	0.97
CI	All cases (*n* = 32)	0.8 ± 0.1	0.8 ± 0.1	0.194
	Sphere (*n* = 12)	0.9 ± 0.1	0.9 ± 0.0	0.248
	Cube (*n* = 10)	0.8 ± 0.1	0.8 ± 0.0	0.323
	Triangular prism (*n* = 10)	0.7 ± 0.0	0.8 ± 0.1	0.279

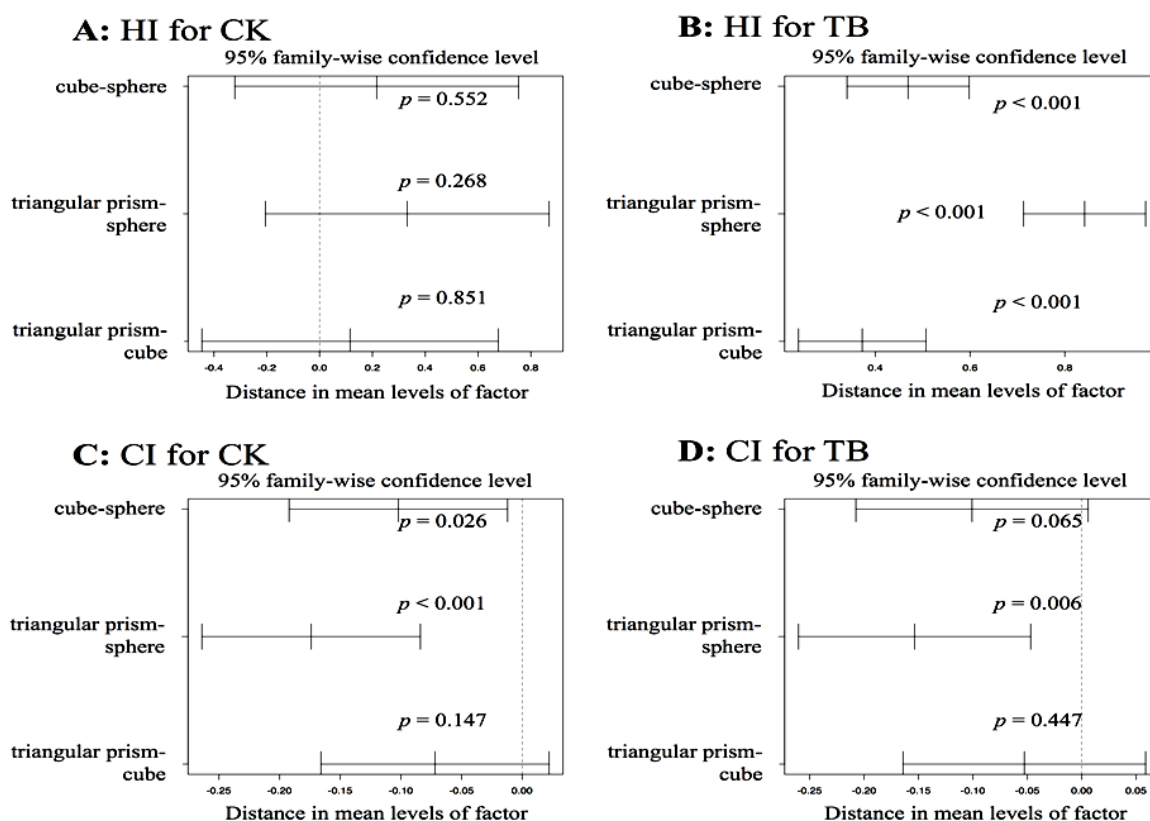CK, CyberKnife; TB, TrueBeam; SD, standard deviation; HI, homogeneity index; CI, conformity index.

Figure 1. HI and CI compared for multiple target shapes for the CK and TB treatment. **(a)** HI for the CK, **(b)** HI for the TB, **(c)** CI for the CK, **(d)** CI for the TB (HI, homogeneity index; CI, conformity index; CK, CyberKnife; TB,

Figure 2 presents the trends observed in the HI and the CI with respect to the target diameter. The HI increased almost monotonically as the target diameter increased (*p* = 0.048) for the CK; however, the association between target diameter and the HI was not remarkable for the TB (*p* = 0.718). Although the CI tended to decrease monotonically as the target diameter increased, there was no significant difference in the CI (*p* = 0.335 and *p* = 0.120 for the CK and TB, respectively).

Figure 3 presents an example of dose distributions from the treatment planning for the CK and TB. Although the area of the target coverage inside the 95% isodose line was similar for each plan, the TB plans showed smooth contours, especially for the angled objects.
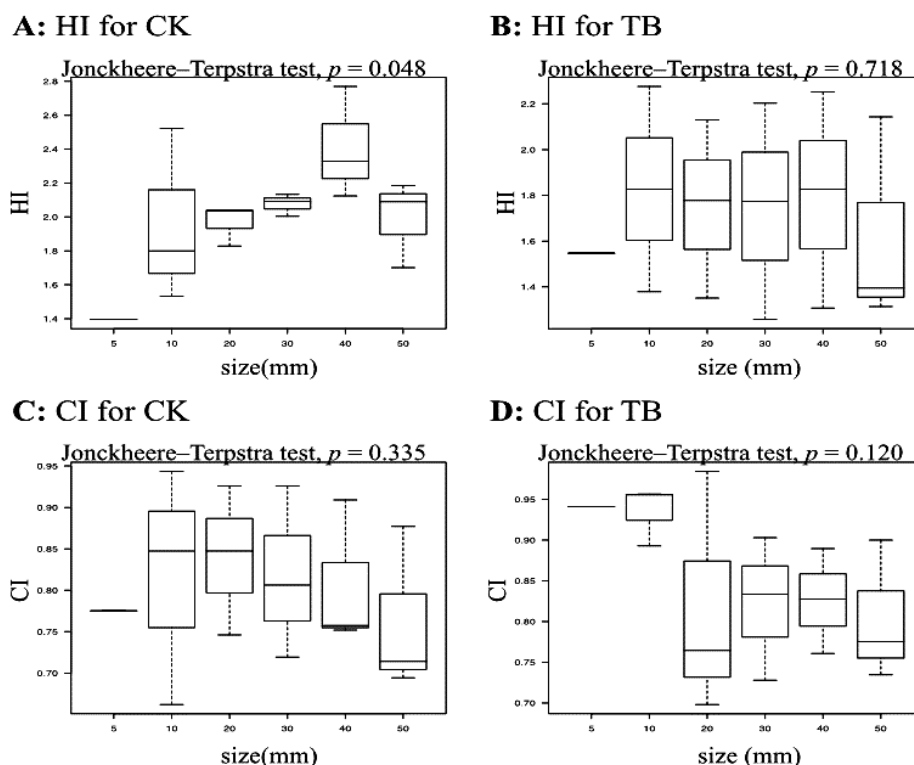
Int. J. Radiat. Res., Vol. 16 No. 4, October 2018

398

Figure 2. HI and CI values as functions of target diameters. **(a)** HI for the CK, **(b)** HI for the TB, **(c)** CI for the CK, **(d)** CI for the TB. (HI, homogeneity index; CI, conformity index; CK, CyberKnife; TB, TrueBeam).
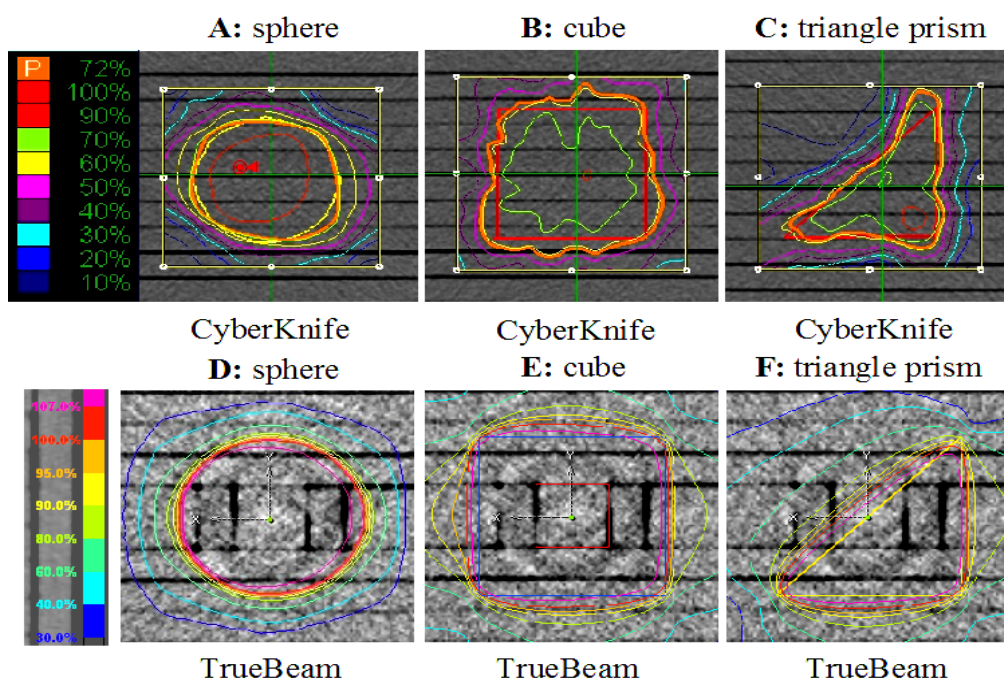

Figure 3. Comparison of dose distributions from the CK and TB treatment. (A-C) Contours for the 50-mm sphere, cube, and triangle prism, respectively, for the CK. (D-F) Contours for the 50-mm sphere, cube, and triangle prism, respectively, for the TB. Although the target coverage of the 95% isodose line (orange line in each panel) was similar in each plan, the TB plans showed smooth contours, especially for angled objects (CK, CyberKnife; TB, TrueBeam).

399

Int. J. Radiat. Res., Vol. 16 No. 4, October 2018

Verification and comparison of dose profiles

Table 3 presents the results of the dose-profile analysis. Flatness was more favourable for the TB compared with the CK (1.4 [range, 1.3–1.7] vs. 1.1 [range, 1.1–1.2]; *p* < 0.001). Although the gradients were favourable for the CK compared with the TB (60 [range, 31–135] vs. 34 [range, 21–108]; *p* < 0.001), there was no difference in the gradients between the CK and the TB for the simple shape (sphere) (54 [range, 41–90] vs. 52 [range, 22–135]; *p* = 0.542). For the CK, the trend in flatness with respect to the target diameter was similar to that of HI, (i.e., it increased monotonically as the target diameter increased, *p* = 0.046). Gradients decreased monotonically as the target diameter increased for both treatment devices (*p* < 0.001).

Table 3. Results of dose profiles along the x- and y-axes at the centre of the irradiated area.

		CK	TB	
		Median (range)	Median (range)	*p* value
Flatness	All cases (*n* = 64)	1.4 (1.3–1.7)	1.1 (1.1–1.2)	<0.001
	Sphere (*n* = 24)	1.6 (1.3–1.7)	1.1 (1.1–1.2)	0.003
	Cube (*n* = 20)	1.3 (1.3–1.6)	1.1 (1.1–1.2)	<0.001
	Triangular prism (*n* = 20)	1.4 (1.4–1.7)	1.1 (1.1–1.2)	<0.001
Gradient	All cases (*n* = 128)	60 (31–135)	34 (21–108)	<0.001
	Sphere (*n* = 48)	52 (22–135)	54 (41–90)	0.542
	Cube (*n* = 40)	42 (26–135)	24 (16–90)	0.022
	Triangular prism (*n* = 40)	84 (68–135)	29 (20–108)	<0.001

CK, CyberKnife; TB, TrueBeam.

DISCUSSION

A previous study reported that DCA irradiation in the LINAC system requires less time than CK irradiation [9]. In this study, the irradiation time was significantly lower with the TB. Although the CK did not carry a multi-leaf collimator, this time reduction was achieved mainly because we used a 6-MV FFF for the TB, which allowed high-rate irradiation of 1400 MU/min. This is advantageous in a clinical setting because stereotactic radiation can be applied to patients who find it difficult to stay in a recumbent position for an extended period. However, the faster treatment times of the TB technology mean there is a much higher integral dose across the targets. Therefore, accurate patient positioning is indispensable to avoid injury to the surrounding normal tissue.

In this study, the HI of the spherical target was better with the TB than with the CK. This difference in HI between modalities became insignificant as the target shape became more complex (cubic or triangular prism). Therefore, we assumed that there was no difference in the HI between the devices when the shape was complex. However, in stratified univariate analysis, the HI decreased (i.e., the dose distribution was not homogeneous) as the target diameter increased for the CK. There was no difference in the CI between the treatment devices. For both treatment devices, the CI values were significantly lower for complex shapes (triangular prism) than for simple ones (sphere). The effect of shape on the CI was similar for both devices. In all cases, as the target diameter increased, the CI tended to decrease monotonically, although the differences in the CI values were not significant. This was most likely because of the small number of samples, which is a result of the stratified nature of this analysis.

Previous studies have compared the CK to the DCA technique for clinical cases [5–10]. Table 4 lists the results of these studies, as well as the findings of our study. The size and shape of the targets varied among the clinical plans of the various studies, although the HI was favourable in arc irradiation, which was consistent with our current results. However, the CI reported in previous studies differed from that reported in

Int. J. Radiat. Res., Vol. 16 No. 4, October 2018

400

the present study, as most reported favourable results for the CK. Dutta *et al.* [10] reported that the CI was similar for both treatment devices when the targets were in close proximity to organs-at-risk. To verify only the physical properties of the 2 devices in the present study, virtual targets were placed at the centre of the phantom and organs-at-risk were not included. It is likely that such variables in the experimental setting were responsible for the difference between our results and those of previous studies.

In our study, the TB had better beam flatness. According to the TB planning system, the HI consistently correlated with the flatness evaluated using the irradiated films. Since it is impossible to calculate the CI from a dose profile, dose convergence was evaluated by defining gradients at the edge of the radiation field. The CK had the better gradient for moderate-to-high doses when the target shape was complex. The gradient results were inconsistent with respect to the CI; however, the gradient results may not always correlate with the CI [11, 14]. Our dose profile verification showed that the results of HI and CI were consistent, but differed from those of other reports [5-9], especially the CI values.

The present study had several limitations, with the most important being the use of different dose calculation algorithms for the 2 modalities. Although we used a phantom consisting of water-equivalent material and the effect of heterogeneity correction seemed to be insignificant, the difference in the management

of scattering may be a limiting factor of this study.

In SRT planning for small targets, the dose gradient around the target and dose homogeneity inside the target are difficult to balance. A more homogeneous plan often has less conformity for target covering and a worse dose gradient for the surrounding normal tissue. Although we carefully balanced the parameters during each treatment plan, it was difficult to define a precise dose prescription.

With regard to HI, some think heterogeneity, namely hot spots in the target, is associated with worse events [15]. In contrast, others think it might be better for tumour control because of the higher tumouricidal effect [16]. Since the purpose of this phantom study was to clarify the physical properties of each device rather than identifying a positive or negative clinical result, we did not consider the clinical relevance of heterogeneity.

In conclusion, the CK is particularly robust for delivering therapeutic radiation to small targets. The TB had a short irradiation time and yielded good results, regardless of target size, when the target morphology was simple. As such, the TB is more suitable for targets with a simple shape or for cases in which the HI is a critical factor. For clinical cases, verification of the target region and its anatomical relationships with organs-at-risk is required; this was not considered in the present study. Nevertheless, we believe our findings provide useful information for future clinical studies.

Table 4. Dosimetric comparison of different treatment modalities for stereotactic radiotherapy from previous studies.

Studies	HI			CI		
	CK	DCA	*p*-value	CK	DCA	*p*-value
Blamek *et al.*[5]	1.2	1.11	<0.05	1.48	1.86	<0.05
Paik *et al.* [6]	1.23	1.1	<0.001	1.05	1.13	<0.001
Treuer *et al.* [7]	NA	NA	NA	0.72	0.57	<0.001
Kaul *et al.* [8]	NA	NA	NA	0.76	0.66	0.002
Gevaert *et al.* [9]	NA	NA	NA	0.77	0.66	<0.01
Dutta *et al.* [10]	NA	NA	NA	0.58	0.53	0.225
Present study	2.1	1.8	0.043	0.8	0.8	0.194

CK, CyberKnife; DCA, dynamic conformal arc; NA, not applicable; HI, homogeneity index; CI, conformity index.

ACKNOWLEDGMENTS

Ethical statement

No human participants or animal experiments were included in this study.

Conflicts of interest: *Declared none.*

REFERENCES

1. Japanese Society for Radiation Oncology. Regular structural survey by JASTRO. [Internet]. 2011 [Cited 2016 May 21]. Available from: http://www.jastro.or.jp/aboutus/datacenter.php.

2. Gallo JJ, Kaufman I, Powell R Pandya S, Somnay A, Bossenberger T, Ramirez E, Reynolds R, Solberg T, Burmeister J (2015) Single-fraction spine SBRT end-to-end testing on TomoTherapy, Vero, TrueBeam, and CyberKnife treatment platforms using a novel anthropomorphic phantom. *J Appl Clin Med Phys, 16: 170-182*.

3. Adler JR, Chang SD, Murphy MJ Doty J, Geis P, Hancock SL (1997) The Cyberknife: a frameless robotic system for radiosurgery. *Stereotact Funct Neurosurg, 69: 124-128*.

4. Scorsetti M, Alongi F, Castiglioni S, Clivio A, Fogliata A, Lobefalo F, Mancosu P, Navarria P, Palumbo V, Pellegrini C, Pentimalli S, Reggiori G, Ascolese AM, Roggio A, Arcangeli S, Tozzi A, Vanetti E, Cozzi L (2011) Feasibility and early clinical assessment of flattening filter free (FFF) based stereotactic body radiotherapy (SBRT) treatments. *Radiat Oncol, 6: 113*.

5. Blamek S, Grzadziel A, Miszczyk L (2013) Robotic radiosurgery versus micro-multileaf collimator: a dosimetric comparison for large or critically located arteriovenous malformations. *Radiat Oncol, 8: 205*.

6. Paik EK, Kim MS, Choi CW, Jang WI, Lee SH, Choi SH, Kim KB, Lee DH (2015) Dosimetric comparison of volumetric modulated arc therapy with robotic stereotactic radiation therapy in hepatocellular carcinoma. *Radiat Oncol, 33: 233-241*.

7. Treuer H, Hoevels M, Luyken K, Visser-Vandewalle V, Wirths J, Kocher M, Ruge M (2015) Intracranial stereotactic radiosurgery with an adapted linear accelerator vs. robotic radiosurgery: Comparison of dosimetric treatment plan quality. *Strahlenther Onkol, 191: 470-476*.

8. Kaul D, Badakhshi H, Gevaert T, Pasemann D, Budach V, Tuleasca C, Gruen A, Prasad V, Levivier M, Kufeld M (2015) Dosimetric comparison of different treatment modalities for stereotactic radiosurgery of meningioma. *Acta Neurochir (Wien), 157: 559-563*.

9. Gevaert T, Levivier M, Lacornerie T, Verellen D, Engels B, Reynaert N, Tournel K, Duchateau M, Reynders T, Depuydt T, Collen C, Lartigau E, De Ridder M (2013) Dosimetric comparison of different treatment modalities for stereotactic radiosurgery of arteriovenous malformations and acoustic neuromas. *Radiother Oncol, 106: 192-197*.

10. Dutta D, Balaji Subramanian S, Murli V, Sudahar H, Gopalakrishna Kurup PG, Potharaju M (2012) Dosimetric comparison of Linac-based (BrainLAB(R)) and robotic radiosurgery (CyberKnife (R)) stereotactic system plans for acoustic schwannoma. *J Neurooncol, 106: 637-642*.

11. Paddick I, Lippitz B (2006) A simple dose gradient measurement tool to complement the conformity index. *J Neurosurg, 105: 194-201*.

12. Oliver M, Chen J, Wong E, Van Dyk J, Perera F (2007) A treatment planning study comparing whole breast radiation therapy against conformal, IMRT and tomotherapy for accelerated partial breast irradiation. *Radiother Oncol, 82: 317-323*.

13. Kanda Y (2013) Investigation of the freely available easy-to-use software "EZR" for medical statistics. *Bone Marrow Transplant, 48: 452-458*.

14. 14. Feuvret L, Noel G, Mazeron JJ, Bey P (2006) Conformity index: a review. *Int J Radiat Oncol Biol Phys, 64: 333-42*.

15. Balagamwala EH, Suh JH, Barnett GH, Khan MK, Neyman G, Cai RS, Vogelbaum MA, Novak E, Chao ST (2012) The importance of the conformality, heterogeneity, and gradient indices in evaluating Gamma Knife radiosurgery treatment plans for intracranial meningiomas. *Int J Radiat Oncol Biol Phys, 83: 1406-1413*.

16. Perks JR, St George EJ, Hamri KE, Blackburn P, Plowman PN (2003) Stereotactic radiosurgery XVI: Isodosimetric comparison of photon stereotactic radiosurgery techniques (gamma knife vs. micromultileaf collimator linear accelerator) for acoustic neuroma—and potential clinical importance. *Int J Radiat Oncol Biol Phys, 57: 1450-1459*.

Int. J. Radiat. Res., Vol. 16 No. 4, October 2018

402